# Partitioning mortality into growth-dependent and growth-independent hazards across 203 tropical tree species

James S. Camac[a,1,2], Richard Condit[b,c], Richard G. FitzJohn[a,3], Lachlan McCalman[d], Daniel Steinberg[d], Mark Westoby[a], S. Joseph Wright[e], and Daniel S. Falster[f]

[a]Department of Biological Sciences, Macquarie University, Sydney, NSW, 2109, Australia; [b]Field Museum of Natural History, Chicago, IL 60605; [c]Morton Arboretum, Lisle, IL 60532; [d]Data61, Commonwealth Scientific and Industrial Research Organisation (CSIRO), Sydney, NSW, 2015, Australia; [e]Smithsonian Tropical Research Institute, Apartado 0843–03092, Balboa, Panama; and [f]Evolution and Ecology Research Centre, School of Biological, Earth and Environmental Sciences, University of New South Wales, Sydney, NSW, 2052, Australia

Edited by William J. Bond, University of Cape Town, Cape Town, South Africa, and approved October 18, 2018 (received for review December 5, 2017)

**Tree death drives population dynamics, nutrient cycling, and evolution within plant communities. Mortality variation across species is thought to be influenced by different factors relative to variation within species. The unified model provided here separates mortality rates into growth-dependent and growth-independent hazards. This model creates the opportunity to simultaneously estimate these hazards both across and within species. Moreover, it provides the ability to examine how species traits affect growth-dependent and growth-independent hazards. We derive this unified mortality model using cross-validated Bayesian methods coupled with mortality data collected over three census intervals for 203 tropical rainforest tree species at Barro Colorado Island (BCI), Panama. We found that growth-independent mortality tended to be higher in species with lower wood density, higher light requirements, and smaller maximum diameter at breast height (dbh). Mortality due to marginal carbon budget as measured by near-zero growth rate tended to be higher in species with lower wood density and higher light demand. The total mortality variation attributable to differences among species was large relative to variation explained by these traits, emphasizing that much remains to be understood. This additive hazards model strengthens our capacity to parse and understand individual-level mortality in highly diverse tropical forests and hence to predict its consequences.**

hazard rates | Bayesian | plant traits | tropical trees | mortality rates

Tree death is a fundamental process affecting population dynamics, nutrient cycling, and evolution within plant communities. While the risk of death varies substantially among forests and from year to year (1), trees growing within the same forest also vary remarkably in realized risk of death (2). In tropical forests, annual mortality can differ 20- to 60-fold among coexisting species (2). This presumably reflects differences in the way trees from different species are constructed and function. Notably there exists a coordinated axis of life-history variation whereby individuals from species with higher potential growth rates also experience higher mortality (3). At the same time the risk of death varies widely within species, with individuals growing slower or sitting lower in the light gradient at higher risk (4–6). In other words mortality increases with growth rate across species, but decreases with growth rate within species. Hence it is important to separate hazards into those connected and unconnected with growth rate and to integrate hazard estimation across and within species.

Although plants die from many causes, our approach described here partitions them into two fundamental categories: growth-dependent hazards and growth-independent hazards (7, 8). Growth-independent hazards cause death irrespective of the tree's current growth rate and may include windfall, fire, and certain types of pathogen or herbivore attack. These hazards are assumed to occur at some average rate (Fig. 1*A*, *Left*). Growth-dependent hazards cause slower-growing plants within each species to die at a faster rate, presumably because inferior carbon budgets make them unable to tolerate diverse stresses (4, 7, 9). Many empirical studies suggest an exponential-like decline in risk with increased growth rate, $X_i(t)$ (4–6) (Fig. 1*A*, *Center*). An individual's total risk of dying is then the sum of growth-independent plus growth-dependent hazards (Fig. 1*A*, *Right*). Biologically, the additive model implies that even fast-growing individuals experience some risk of death.

The additive hazards model has not previously been applied for empirical analysis, although it has been adopted in some vegetation models (10). In most previous empirical studies the underlying mathematical structure of statistical methods used

## Significance

**We present a model that partitions rates of tropical tree mortality into growth-dependent and growth-independent hazards. This creates the opportunity to examine the relative contributions of within-species and across-species variation on tropical tree mortality rates, but also how species traits affect each hazard. We parameterize this model using >400,000 observed survival records collected over a 15-y period at Barro Colorado Island, Panama from more than 180,000 individuals across 203 species. We show that marginal carbon budgets are a major contributor to tree death on Barro Colorado Island. Moreover, we found that while species' light demand, maximum diameter at breast height (dbh), and wood density affected tree mortality in different ways, they explained only a small fraction of the total variability observed among species.**

Author contributions: J.S.C., R.C., R.G.F., L.M., D.S., M.W., S.J.W., and D.S.F. designed research; J.S.C. and D.S.F. performed research; J.S.C. and D.S.F. contributed new reagents/analytic tools; J.S.C., R.G.F., and D.S.F. analyzed data; J.S.C., M.W., and D.S.F. wrote the paper; and R.C. and S.J.W. collected data.

The authors declare no conflict of interest.

This article is a PNAS Direct Submission.



Data deposition: Code reproducing the results in this paper has been deposited on figshare at https://doi.org/10.6084/m9.figshare.7295486.v1. Data from BCI are available at DOIs 10.5479/data.bci.20130603 and 10.5479/data.bci20140711. A copy of the R code used to construct the Barro Colorado Island mortality model can also be found at the following GitHub repository: https://github.com/traitecoevo/mortality_bci.

[1]To whom correspondence should be addressed. Email: james.camac@gmail.com.

[2]Present address: Center of Excellence for Biosecurity Risk Analysis, School of Biological Sciences, The University of Melbourne, Melbourne, VIC, 3010, Australia.

[3]Present address: Department of Infectious Disease Epidemiology, Imperial College London, Faculty of Medicine, London W2 1PG, United Kingdom.

This article contains supporting information online at www.pnas.org/lookup/suppl/doi:10.1073/pnas.1721040115/-/DCSupplemental.

Published online November 16, 2018.





ECOLOGY

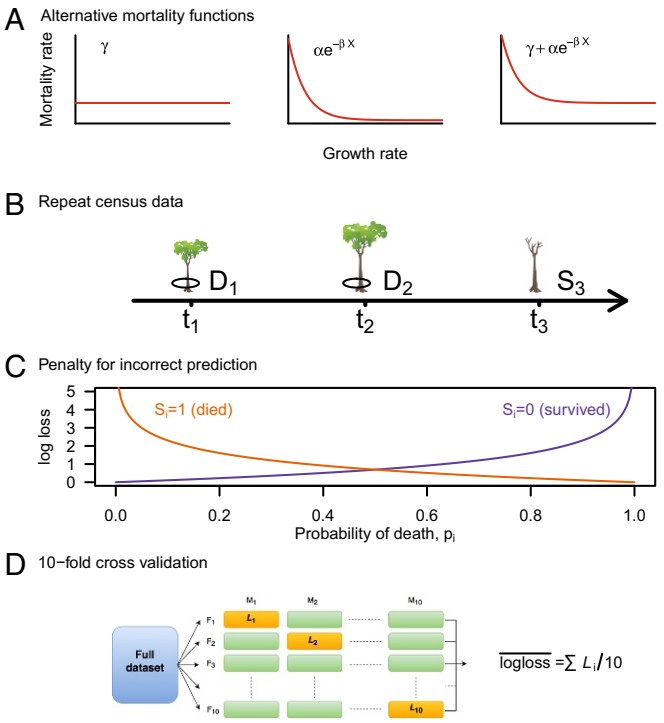


**Fig. 1.** Outline of methodology. (*A*) We consider three alternative hazard functions: (*i*) a growth-independent baseline hazard (*Left*); (*ii*) a growth-dependent hazard, where growth rate is a proxy for carbon budget (*Center*); and (*iii*) a function that combines growth-dependent with growth-independent hazards (*Right*). The parameters of the models are biologically interpretable: $\gamma$ is the baseline or growth-independent hazard, $\alpha$ defines the low growth rate (i.e., very marginal carbon budget) effect on the overall hazard, and $\beta$ captures the sensitivity or curvature of the response to declining growth rate. In the most complex model (*A*, *Right*), $\alpha$ and $\beta$ capture growth-dependent hazards, while $\gamma$ captures growth-independent hazards that kill a plant, irrespective of its growth rate/carbon budget (e.g., windfall, fire). For each model form, we consider two alternative measures of growth, $X$ (basal area and stem diameter growth), and we allow for species-level effects on the parameters $\alpha$, $\beta$, and $\gamma$. (*B*) Our data consist of repeat measures of stem diameter (*D*) and status (*S*, 0 = alive or 1 = dead) for individual trees at specific census dates ($t_1$, $t_2$, $t_3$). Tree illustration courtesy of Tracey Saxby, Integration and Application Network, University of Maryland Center for Environmental Science (ian.umces.edu/imagelibrary/). (*C*) Each model's skill in predicting observed outcomes (*S*) is quantified via the log-loss function (Eq. **4**). Lower log loss means higher predictive accuracy. (*D*) The predictive accuracy of alternative models was evaluated via 10-fold cross-validation. The entire dataset is split into 10-folds ($F_1$, . . ., $F_{10}$). Alternative models were fitted 10 times ($M_1$, . . ., $M_{10}$), using different combinations of testing (1-fold; orange) and training (9-fold; green) data. Predictive accuracy was assessed by averaging the log loss obtained from the 10 test data predictions.

implies responses similar to those of either Fig. 1*A*, *Left* or Fig. 1*A*, *Center* (*SI Appendix*). In particular, the commonly used exponential models (4, 5), logistic regression (11), generalized linear models (12), and Cox proportional-hazard models (13) handle covariates in a manner that allows predicted risk to decline to zero for fast-growing individuals (as in Fig. 1*A*, *Center*) (*SI Appendix*). This makes these methods less likely to capture the full range of variation within and among species.

## An Additive Hazards Model with Species Effects

Forest mortality rates are usually estimated from census data, where the size and alive vs. dead status of individual trees are recorded at successive time points (14) (Fig. 1*B*). From these data one can estimate $\lambda_i(t)$, a continuous, latent mortality rate or hazard rate for each individual, $i$, at time $t$. The probability an individual dies between times $t_1$ and $t_2$ results from the cumulative hazard they are exposed to between censuses (15):

$$p_{i,t_1\to t_2} = 1 - \exp\left(-\int_{t_1}^{t_2} \lambda_i(t)\,\mathrm{d}t\right). \quad [1]$$

The observed survival outcome $S_{i,t_1\to t_2}$ (0 = alive, 1 = died) is then modeled as a binary draw from $p_{i,t_1\to t_2}$. The challenge is then to estimate an appropriate form for the hazard rate, $\lambda_i(t)$.

Here we propose the following hazard function, incorporating individual-, species-, and census-period effects:

$$\lambda_i(t) = \left(\overbrace{\gamma_s}^{\text{Growth independent}} + \overbrace{\alpha_s\, e^{-\beta_s X_i(t)}}^{\text{Growth dependent}}\right) \times \overbrace{\delta_t}^{\text{Census}}. \quad [2]$$

Eq. **2** allows for additive growth-dependent and growth-independent effects, includes a negative exponential effect of the individual's growth rate ($X$; our measure of carbon budget), allows the overall mortality rate to vary among censuses via the random effect $\delta_t$, and also provides for species-level differences in the shape of $\lambda_i(t)$ via the parameters $\alpha_s$, $\beta_s$, and $\gamma_s$. The species-level parameters are in turn modeled as a function of both species trait effects and species-level random effects, the latter of which accounts for residual species variation not attributed to traits.

A further advantage of the proposed hazard function (Eq. **2**) is that it allows us to estimate (at population level) the relative contributions of different mortality events, even if the causes of death for each individual tree remain unknown.

To illustrate the proposed mortality model, we assess its ability to predict the survival status of 180,503 individual trees from 203 species, recorded over three 5-y census periods at Barro Colorado Island (BCI), Panama. Applying the additive model, we (*i*) estimate growth-dependent and growth-independent effects from long-term census data, (*ii*) estimate species-level differences in these effects, and (*iii*) assess how well species-level differences are predicted from three fundamental traits, previously shown to correlate with mortality: wood density, light demand, and maximum diameter at breast height (dbh) (3, 11, 16, 17). These traits show only weak correlation with each other ($r^2 < 0.13$) and thus provide relatively independent measures of a species ecological strategy (*SI Appendix*, Fig. S7).

Using a likelihood-based penalty for incorrect prediction, we used 10-fold cross-validation to evaluate the skill of different models in their ability to predict outcomes in novel data (i.e., not used in model fitting; Fig. 1 *C* and *D* and *Materials and Methods*) (18, 19). In total 427,460 observations were used to fit these models. Evaluating models in this way is computationally expensive. Therefore, rather than running all possible model formulations, we fitted models across six levels of increasing complexity, described below, and compared their predictive accuracy. We then used the final model to assess the effects of species traits on each parameter and quantify their relative contributions on the overall model performance. Relative contributions of parameters were assessed using $r^2$ and area under the ROC receiver curve (AUROC). Thereby, $r^2$ estimates were derived from modeled predictions vs. proportion of individual deaths observed between 1995 and 2010 for each species and thus measured the amount of species-level variation explained by the model (12). By contrast, AUROC examined the model's ability to distinguish individuals that died from individuals that survived, irrespective of species.

## Results

**Stage 1: Mortality Over Time.** We first assess whether average mortality rates varied among the three censuses, in other words whether a census effect is justified in Eq. **2**. Comparing a model with a constant mortality rate $\gamma$ to a model where the constant is scaled by a census effect $\gamma\delta_t$ and examining the three 5-y census intervals, average mortality rates declined over time. The highest proportion of deaths occurred from 1995 to 2000 (16%) followed by 2000–2005 (13%) and 2005–2010 (12%). Consequently, we observed a small increase in predictive accuracy when a census effect was included [leftmost two points (open circles) under stage 1 in Fig. 2; see also Table 1 for quantification of gain in predictive power under successive models].

**Stage 2: Hazard Functions.** Second, we assessed the predictive accuracy of three alternative hazard functions (Fig. 1*A*). The simplest form (Fig. 1*A*, *Left*) assumes a constant hazard. The second form (Fig. 1*A*, *Center*) assumes the risk of dying declines toward an asymptote of zero as growth increases. The third "additive" model (Fig. 1 *A* and *B*, *Right*) is the sum of the previous two. In parallel, we investigated also which growth measure (increment of stem diameter or of stem area) predicts growth-dependent mortality better. Comparing the three hazard functions, the additive function significantly outperformed both the baseline (the best model in stage 1) and growth-dependent–only hazard functions (right vs. left of the four symbols under stage 2 in Fig. 2). Predictive accuracy was higher when using stem-diameter growth compared with stem-area growth (Fig. 2, stage 2, shaded vs. solid symbols).

**Stages 3–5: Species Traits.** In stages 3–5, we take the additive model using dbh growth rate (the most predictive hazard function and growth rate measure from stage 2) and ask how addition of one, two, and three species-level traits improves model performance. Specifically, we introduce effects of the traits maximum dbh ($\psi$), light demand ($\upsilon$), and wood density ($\rho$) on the parameters $\alpha$, $\beta$, and $\gamma$ in Eq. **2**, at first one at a time (stage 3) and then in two-trait (stage 4) and three-trait (stage 5) combinations. In general we found that including trait effects on these parameters decreased logarithmic loss and, thus, increased predictive accuracy (Fig. 2). Allowing all three traits to have an effect on these parameters resulted in higher predictive accuracy relative to that in models that incorporated only one or two of the traits.

**Stage 6: Species Random Effects and Trait Effects.** To examine how species differed in hazard functions and to understand the effects of species traits, we used the entire dataset to fit a final model containing all three species traits plus a species random effect to capture interspecific variation not explained by traits. The increase in predictive accuracy afforded by traits (Fig. 2, compare best model at stage 2 with stage 5) was fairly small relative to including species random effects on each parameter (Fig. 2, compare stages 5 and 6), signifying that substantial interspecific variation in mortality rates remains unexplained.

Each trait influenced tree mortality in different ways (Figs. 3 and 4). Light-demanding species were more susceptible to low growth rates (i.e., higher $\alpha$), had higher growth-independent hazards (i.e., higher $\gamma$), and exhibited shallower declines in growth-dependent hazards with increasing growth rates (i.e., lower $\beta$). Wood density had significant impacts on $\alpha$ and $\gamma$, such that species with high wood density were less susceptible to low growth rates and had lower growth-independent hazards. Species' maximum dbh had significant effects only on $\gamma$, whereby species capable of achieving larger dbh exhibited lower growth-independent hazards. All parameter estimates for the final model are in *SI Appendix*, Tables S1 and S2.

**Explanatory Power.** The full model had an AUROC of 0.722, indicating a fair ability to correctly discriminate observed deaths from survivals. Moreover, we found that the full model also explained 98.5% of the total variation in mortality observed among species.

Removal of the census random effect $\delta_t$ had little impact on either $r^2$ or AUROC. The removal of either wood density or light demand resulted in similar magnitude effects on both $r^2$ and AUROC. By contrast, the removal of maximum dbh had a slightly smaller effect on both metrics. Both $r^2$ and AUROC dropped substantially when species random effects were removed, further highlighting that maximum dbh, light demand, and wood density explain only a small fraction of the overall interspecific variation observed among species. When both species traits and species random effects were removed, the resulting model was by definition unable to capture any

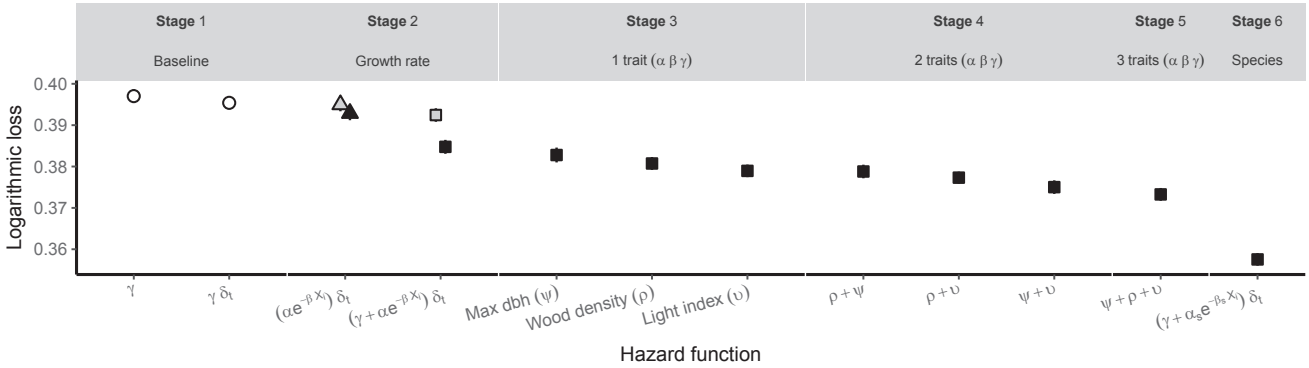


**Fig. 2.** Predictive accuracy of alternative hazard functions. Values are mean (±95% confidence intervals) logarithmic loss, with lower values implying greater predictive accuracy and a log loss ≈0.693 indicating a model unable to distinguish an observed death from a survival. Shown are six sequential stages of model selection with each stage increasing in complexity. Stage 1: Baseline: constant ($\gamma$) vs. baseline with census effect ($\gamma\,\delta_t$). Stage 2: Best model of stage 1 compared with hazard functions that also account for individual growth rate (i.e., carbon budget). This includes two possible hazard functions: a growth-dependent–only hazard ($(\alpha e^{-\beta X_i})\delta_t$) and a baseline + growth-dependent hazard with census effects ($(\alpha e^{-\beta X_i}+\gamma)\delta_t$. Stage 3: The effect of a species' maximum dbh ($\psi$), wood density ($\rho$), and light demand ($\upsilon$) on $\alpha$, $\beta$, and $\gamma$ of the most predictive model from stage 2. Stage 4: Two-trait combinations. Stage 5: Three-trait combination. Stage 6: Maximum predictive performance by accounting for all species differences via the inclusion of species random effects, *s* on all three parameters. Symbols represent the three hazard functional forms: baseline (circle), growth dependent (triangle), and containing both growth-independent and growth-dependent hazards (square). Shadings represent models that do not account for individual growth (open circles), use individual basal area growth (shaded square and triangle), or use diameter increment growth (solid triangle and squares).

**Table 1. Relative effects of parameter removal on both $r^2$ and AUROC**

| Model | $r^2$ | AUROC |
|---|---|---|
| Full model | 0.985 | 0.722 |
| Full minus census error | 0.979 | 0.718 |
| Full minus wood density | 0.823 | 0.711 |
| Full minus light demand | 0.829 | 0.713 |
| Full minus max dbh | 0.889 | 0.716 |
| Full minus species error | 0.330 | 0.668 |
| Full minus species traits and species error | 0.000 | 0.635 |
| Full minus growth-dependent hazard | 0.795 | 0.640 |
| Full minus growth-independent hazard | 0.653 | 0.703 |

$r^2$ estimates are derived from modeled predictions vs. proportion of individual deaths observed between 1995 and 2010 for each species. As such, $r^2$ measures the amount of species-level variation explained by the model or submodels. By contrast, AUROC examines the model's ability to distinguish individuals that died from individuals that survived, irrespective of species.

variation observed among species and thus had low discriminatory ability. Finally, we found the removal of the growth-independent hazard term ($\gamma_s$) resulted in a lower $r^2$ relative to the removal of the growth-dependent hazard ($\alpha_s e^{-\beta_s X_i}$), indicating that the former hazard explained more interspecific variation. However, when examining the removal of these hazards in terms of the model's ability to correctly distinguish survivors from those that died (AUROC), we found the opposite—that the removal of the growth-dependent hazard resulted in substantially lower predictive ability.

## Discussion

Our Bayesian framework coupled with cross-validation revealed that the most predictive hazard model of tropical tree death was one which (*i*) partitioned mortality into growth-dependent and growth-independent hazards; (*ii*) used stem-diameter growth rather than basal-area growth; (*iii*) included the effects of species' maximum dbh, wood density, and light demand; and (*iv*) incorporated temporal variability. Further, rates of tropical tree mortality varied substantially between species and a species' maximum dbh, wood density, and light demand explained only a fraction of the overall interspecific variation.

There are several distinct advantages to modeling tree mortality as a function of two additive hazards: (*i*) The model explicitly accounts for the independent effects of the two fundamental types of hazards faced by plants; (*ii*) it allows for the examination of the relative contributions each hazard provides to the overall hazard rate; (*iii*) it allows for examination of how various factors affect each hazard term; and, because of this, (*iv*) it allows ecological theories of how factors such as species traits affect plant mortality to be empirically tested using commonly collected data.

The findings of this study provide empirical support for dynamic vegetation models that predict tree mortality as a function of both growth-dependent and -independent hazards (8, 10, 20). Regardless of growth measure (our proxy for carbon budget), incorporating both hazards significantly improved model predictive accuracy. This was because the growth-dependent hazard allows for deaths associated with low carbon budgets and, as a consequence, incorporates intraspecific variability attributed to carbon-related stresses such as competition, parasites, and herbivory. By contrast, the growth-independent hazard accounts for deaths caused by events that arise irrespective of an individual's carbon budget such as windthrow or lightning strike.

Partitioning mortality rates into growth-dependent vs. growth-independent effects allowed us to estimate not only their relative contribution, but also how species traits affect each. Like many other studies (11, 16, 21, 22), our analyses highlighted the importance of light competition for tropical tree demographic rates. Specifically, removal of the growth-dependent hazard term resulted in a substantial reduction in the model's ability to

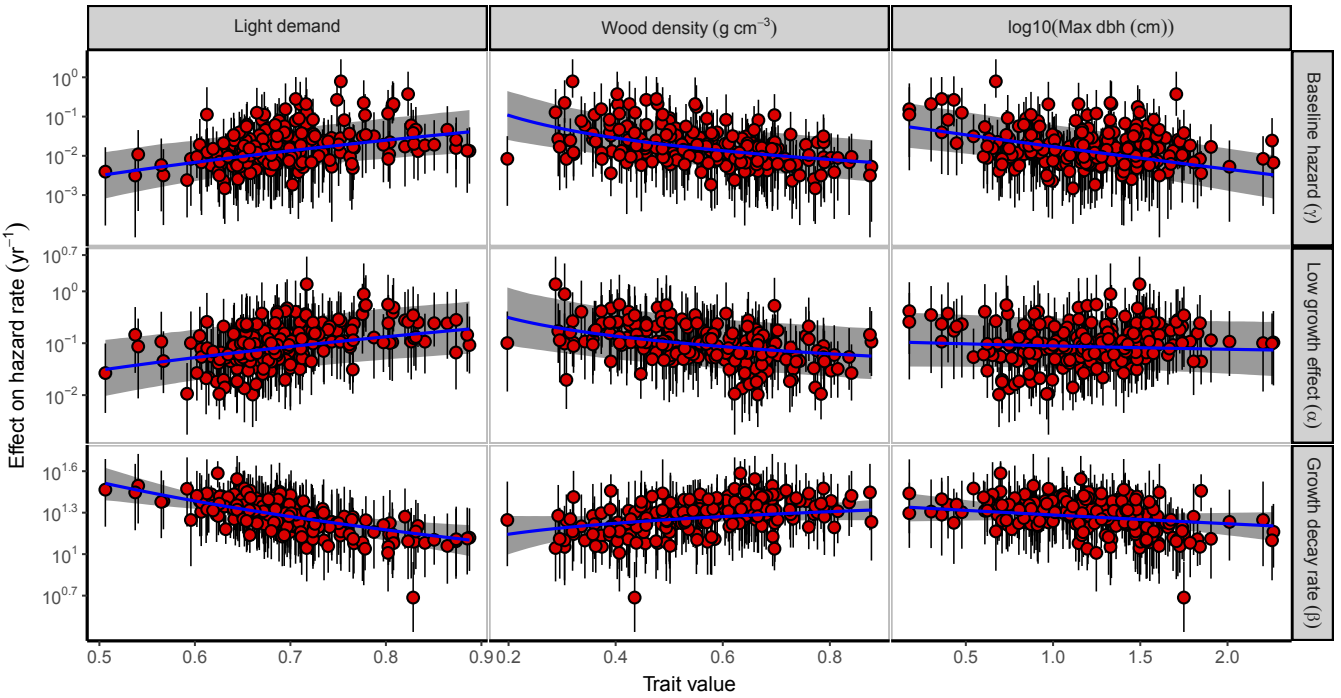


**Fig. 3.** Estimated relationships between species traits (maximum dbh, light demand, and wood density) and model parameters $\alpha$ (low growth effect), $\beta$ (growth-mortality decay rate), and $\gamma$ (baseline/growth-independent hazard). Points are the estimated mean (±95% credible intervals) parameters for each of the 203 Barro Colorado Island species used in this study. Blue trendline with gray shading shows average (±95% credible intervals) expected relationship across observed trait ranges.

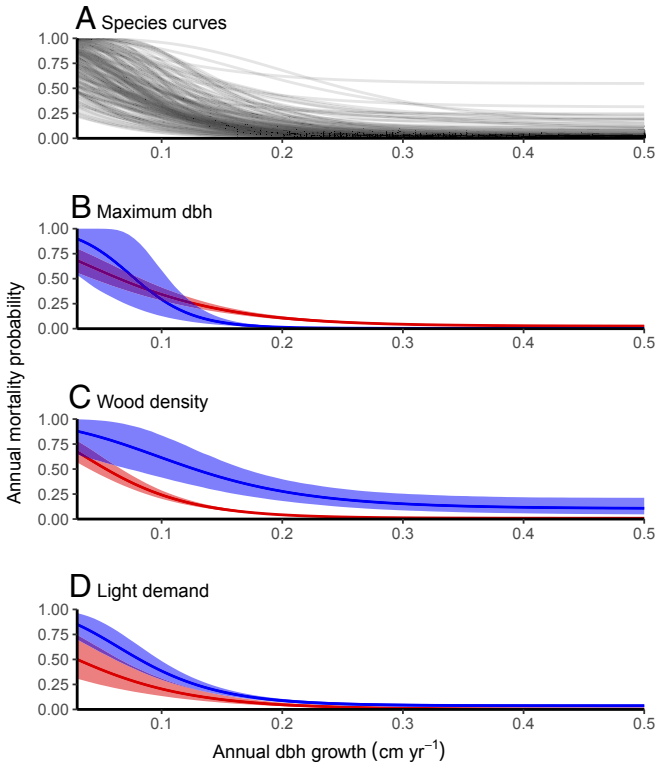


**Fig. 4.** Predicted changes in annual mortality probability with increasing growth rate. (*A*) Estimated average curves for all 203 Barro Colorado Island species used in this study. (*B–D*) The average (±95% credible intervals) curve for a high (red) and a low (blue) trait value. (*B*) Maximum dbh values 3 cm vs. 180 cm. (*C*) wood density values 0.2 g · cm$^{-3}$ vs. 0.8 g · cm$^{-3}$. (*D*) Light demand values 0.5 vs. 0.8. Note that the intercept is the sum of $\alpha$ and $\gamma$ (i.e., the stochastic chance of death plus effect of low growth). The species with highest asymptote in *A* was *Palicourea guianensis* where 561 of 611 individuals died between 1995 and 2010. See *SI Appendix*, Fig. S1 for equivalent hazard curves.

correctly distinguish survivors from those that died (Table 1). This suggests marginal carbon budgets are a major contributor to tree death on Barro Colorado Island. Specifically, the mortality rate for individuals in most species increased substantially once diameter growth rates dropped below 0.1 cm/y (Fig. 4).

Our analyses support previous research that advocated that wood density, species maximum size, and light demand are important explanatory variables of interspecific variation in tropical rainforests (16, 23, 24). Specifically, we show that light-demanding species not only are more susceptible to both low growth rates and growth-independent hazards, but also exhibited shallower declines in growth-dependent hazards with increasing growth rates. By contrast, high maximum-dbh and high wood density species were found to be more tolerant of growth-independent hazards, corroborating evidence reported elsewhere (17, 24). Our analyses also support other work (22, 25) showing that higher wood density species tend also to be more tolerant of low growth rates and better able to tolerate shade and competition.

Basal area growth is thought to be intrinsically linked to changes in total leaf area (26) and thus a better predictor of tree mortality. However, we found the opposite—past diameter growth better predicted tropical tree mortality relative to past basal-area growth. This finding may be due to diameter growth being more variable among smaller, more vulnerable, tree sizes (*SI Appendix*, Fig. S8) and thus better able to capture size-dependent mortality. We did not directly account for individual size in our additive hazards model. This was because of two main reasons: (*i*) Size is highly correlated with both measures of growth (Pearson correlations up to 75%; *SI Appendix*, Fig. S8) and consequently is prone to parameter identifiability issues where the model is unable to discern growth from size effects, and (*ii*) the effect of size is highly nonlinear (6, 11), and thus its inclusion and subsequent interpretation would not be straightforward. Further work is required to determine the independent effects of size and growth effects on tree mortality, but also how to partition size effects between growth-dependent and growth-independent hazards.

Effects of species' wood density, maximum size, and light demand are now being incorporated into mortality algorithms within many vegetation models in the effort to account for among-species variation (10, 27). However, the present analysis indicates that such traits are likely to capture only a small proportion of the overall interspecific variation (Fig. 4 and Table 1). This means that dynamic vegetation models incorporating these traits are likely to account for a fraction of the true variability in tropical rainforest mortality rates and as a consequence underestimate carbon, water, and nutrient dynamics of ecosystems (28).

## Materials and Methods

**Data.** We derived plant mortality models using individual growth and survival data collected from a relatively undisturbed 50-ha tropical rainforest plot on BCI, Panama (9.15° N, 79.85° W). The climate on the island is warm and rainfall is seasonal with most falling between April and November (29).

Within the 50-ha plot the diameter at breast height and survival status of all free-standing woody plants that were at least 1.3 m tall and had diameter ≥1 cm were recorded in 1981–1983, 1985, and every 5 y thereafter (29). For the purpose of modeling mortality as a function of past growth, we discarded data collected before 1990. This was because diameter measurements were rounded to the nearest 5 mm for individuals with dbh < 55 mm, whereas in later censuses all individuals were measured to the nearest millimeter (30). Consequently, we modeled tree mortality as a function of past growth (our measure of available carbon budget) for censuses 1995–2000, 2000–2005, and 2005–2010. We discarded species that do not exhibit secondary growth (e.g., palms and ferns), contained fewer than 10 individuals, or where estimated wood density was not available. We also excluded individuals that (*i*) did not survive at least two censuses (two being required to estimate growth rate), (*ii*) were not consistently measured at 1.3 m above ground, (*iii*) were multistemmed, (*iv*) resprouted or seemingly "returned from the dead," or (*v*) were extreme outliers—stems which grew more than 5 cm · y$^{-1}$ or shrunk more than 25% of their initial diameter. In total 427,460 observations were used in this study comprising 180,503 individual trees and 203 species. Because of computational costs, the models fitted in this study do not include individual random effects. Instead, our models assume that repeat measurements of an individual are independent of one another. We believe this is a reasonable assumption given there were ∼5 y between censuses.

Wood density for each species was estimated by coring trees located within 15 km of the BCI plot (3). Cores were broken into pieces, each 5 cm long, and specific gravity of each piece was determined by oven drying (100 °C) and dividing by the fresh volume (measured by water displacement).

A species' light demand was calculated using annual canopy census data collected during 1985–1990 and 1990–1995. The canopy census recorded, in all 5 5-m subplots across the 50-ha plot, the presence of leaf in six height intervals (0–2 m, 2–5 m, 5–10 m, 10–20 m, 20–30 m, >30 m). The light demand for each species was estimated as the mean light index encountered by new saplings appearing in the census, as described in *SI Appendix* (also *SI Appendix*, Fig. S3).

A species' maximum dbh was estimated directly from the data by taking the 95th percentile observed for each species.

**Model Fitting.** Eqs. **1** and **2** were fitted to the data with covariates for growth rate in previous census, species traits—maximum dbh, light demand, and wood density, as well as random effects for both species and census period. Growth rates were estimated from field measurements of diameter, which inevitably include observation error. In our dataset, 8% of estimated growth rates were negative. To ensure our mortality model was not biased by these unlikely values we first applied a probabilistic model to estimate

"true growth," taking into account measurement error and the distribution of growth rate across the community (*SI Appendix* text and *SI Appendix*, Fig. S1). The parameters $\alpha_s$, $\beta_s$, and $\gamma_s$ were modeled as a function of species traits—maximum dbh $\psi$, wood density $\rho$, and light demand $\upsilon$—and a species-level random effect

$$\alpha_s = \alpha_{0,s}\left(\frac{\rho}{0.6}\right)^{\alpha_1}\left(\frac{\upsilon}{0.7}\right)^{\alpha_2}\left(\frac{\psi}{15}\right)^{\alpha_3}, \quad [3]$$

with similar formulations for $\beta_s$ and $\gamma_s$. Here $\alpha_1$ is the effect of wood density $\rho$, $\alpha_2$ is the effect of light demand $\upsilon$, and $\alpha_3$ is the effect of maximum dbh $\psi$. $\alpha_{0,s}$ captures any other species-level residual error that is otherwise not explained by these three species traits. These random effects were modeled as random realizations from log-normal distributions. The form of Eq. **3** ensures that parameters remain positive; and on a log scale this equates to an additive linear model centered around the denominator. In this case we centered wood density on 0.6 $g \cdot cm^{-3}$, light demand on 0.7, and maximum dbh on 15 cm. We also centered growth rate $X_i$ at the lower 5% quantile for both diameter increment and area growth (0.172 and 0.338, respectively), meaning $\alpha_s$ should be interpreted as the hazard rate when growth rate was very low. Weak priors on all hyperparameters were set (*SI Appendix*). Models were fitted in R 3.5.0 using the package rstan 2.17.3 (31) and using some numerical optimizations (*SI Appendix*). We executed three independent chains and in all cases modeled parameters converged within 2,000 iterations. Convergence was assessed through both visual inspection of chains and reference to the Brooks–Gelman–Rubin convergence diagnostic (32). After discarding the first 1,000 iterations as "burn in," a further 1,000 iterations were taken from the joint posterior. All parameter estimates from the final model are provided in *SI Appendix*, Tables S1 and S2 and Figs. S4–S6.

**Evaluating Model Predictive Accuracy.** Predictive accuracy was quantified by estimating the average log loss across 10-folds for held-out data, $\bar{\mathcal{L}}$ (Fig. 1). Logarithmic loss—commonly known as log loss, $\mathcal{L}$, measures the accuracy of a model by penalizing incorrect predictions, based on how wrong the predicted probability is from the observed outcome, $S_i$ (Fig. 1C). Lower $\mathcal{L}$ implies greater accuracy. The average log loss across all individuals for the $k$th-fold of held-out data, $\mathcal{L}_k$, is then

$$\mathcal{L}_k = -\frac{1}{N_k}\sum_{i=1}^{N_k}\left(S_i\ \log(p_{i,t_2\to t_3}) + (1-S_i)\ \log(1-p_{i,t_2\to t_3})\right), \quad [4]$$

where $N_k$ refers to the number of observations in each fold.

**ACKNOWLEDGMENTS.** We thank H. Muller-Landau, Peter Vesk, and anonymous reviewers for feedback and B. Carpenter for technical advice. We acknowledge S. Hubbell, R. Foster, R. Pérez, S. Aguilar, S. Lao, S. Dolins, and hundreds of field workers for their contribution and the National Science Foundation, Smithsonian Tropical Research Institute, and MacArthur Foundation for funding the design, collection, quality control, and management of long-term growth data at BCI. J.S.C., R.G.F., L.M., and D.S. were supported by the Science and Industry Endowment Fund (RP04-174). D.S.F. and M.W. were supported by fellowships from the Australian Research Council.

1. van Mantgem PJ, et al. (2009) Widespread increase of tree mortality rates in the Western United States. *Science* 323:521–524.
2. Condit R, et al. (2006) The importance of demographic niches to tree diversity. *Science* 313:98–101.
3. Wright SJ, et al. (2010) Functional traits and the growth–mortality trade-off in tropical trees. *Ecology* 91:3664–3674.
4. Kobe RK, Pacala SW, Silander JA (1995) Juvenile tree survivorship as a component of shade tolerance. *Ecol Appl* 5:517–532.
5. Wyckoff PH, Clark JS (2000) Predicting tree mortality from diameter growth: A comparison of maximum likelihood and Bayesian approaches. *Can J For Res* 30:156–167.
6. Vieilledent G, Courbaud B, Kunstler G, Dhôte JF (2010) Mortality of silver fir and Norway Spruce in the Western Alps – a semi-parametric approach combining size-dependent and growth-dependent mortality. *Ann For Sci* 67:305–305.
7. Keane RE, et al. (2001) Tree mortality in gap models: Application to climate change. *Clim Change* 51:509–540.
8. McDowell NG, et al. (2011) The interdependence of mechanisms underlying climate-driven vegetation mortality. *Trends Ecol Evol* 26:523–532.
9. Hawkes C (2000) Woody plant mortality algorithms: Description, problems and progress. *Ecol Model* 126:225–248.
10. Moorcroft PR, Hurtt GC, Pacala SW (2001) A method for scaling vegetation dynamics: The ecosystem demography model (ED). *Ecol Monogr* 71:557–586.
11. Rüger N, Huth A, Hubbell SP, Condit R (2011) Determinants of mortality across a tropical lowland rainforest community. *Oikos* 120:1047–1056.
12. Visser MD, et al. (2016) Functional traits as predictors of vital rates across the life cycle of tropical trees. *Funct Ecol* 30:168–180.
13. Neumann M, Mues V, Moreno A, Hasenauer H, Seidl R (2017) Climate variability drives recent tree mortality in Europe. *Glob Change Biol* 23:4788–4797.
14. Anderson-Teixeira KJ, et al. (2015) CTFS-ForestGEO: A worldwide network monitoring forests in an era of global change. *Glob Change Biol* 21:528–549.
15. Kleinbaum DG, Klein M (2012) *Survival Analysis, A Self-Learning Text*, eds Gail M, Krickeberg K, Samet JM, Tsiatis A, Wong W (Springer, New York), 3rd Ed.
16. King DA, Davies SJ, Sylvester T, Supardi MNN (2006) The role of wood density and stem support costs in the growth and mortality of tropical trees. *J Ecol* 94:670–680.
17. Kraft NJB, Metz MR, Condit RS, Chave J (2010) The relationship between wood density and mortality in a global tropical forest data set. *New Phytol* 188:1124–1136.
18. Hooten MB, Hobbs NT (2015) A guide to Bayesian model selection for ecologists. *Ecol Monogr* 85:3–28.
19. Stone M (1997) An asymptotic equivalence of choice of model by cross-validation and Akaike's criterion. *J R Stat Soc B* 39:44–47.
20. Pacala SW, Canham CD, Saponara J, Kobe RK, Ribbens E (1996) Forest models defined by field measurements: Estimation, error analysis and dynamics. *Ecol Monogr* 66:1–43.
21. King DA (1994) Influence of light level on the growth and morphology of saplings in a Panamanian forest . *Am J Bot* 81:948–957.
22. Kunstler G, et al. (2016) Plant functional traits have globally consistent effects on competition. *Nature* 529:204–207.
23. Poorter L, Bongers L, Bongers F (2006) Architecture of 54 moist-forest tree species: Traits, trade-offs, and functional groups. *Ecology* 87:1289–1301.
24. Chave J, et al. (2009) Towards a worldwide wood economics spectrum. *Ecol Lett* 12:351–366.
25. van Gelder HA, Poorter L, Sterck FJ (2006) Wood mechanics, allometry, and life-history variation in a tropical rain forest tree community. *New Phytol* 171:367–378.
26. Falster DS, Duursma RA, FitzJohn RG (2018) How functional traits influence plant growth and shade tolerance across the life cycle. *Proc Natl Acad Sci USA* 115:E6789–E6798.
27. Scheiter S, Langan L, Higgins SI (2013) Next-generation dynamic global vegetation models: Learning from community ecology. *New Phytol* 198:957–969.
28. Johnson M, et al. (2016) Variation in stem mortality rates determines patterns of aboveground biomass in Amazonian forests: Implications for dynamic global vegetation models. *Glob Change Biol* 22:3996–4013.
29. Condit R, et al. (2012) Barro Colorado forest census plot data, 2012. Available at https://repository.si.edu/handle/10088/20925. Accessed October 31, 2018.
30. Condit R, Pérez R, Lao S, Aguilar S, Hubbell SP (2017) Demographic trends and climate over 35 years in the Barro Colorado 50 ha plot. *For Ecosyst* 4:17.
31. Stan Development Team (2018) RStan: The R interface to Stan. R package version 2.17.3. Available at mc-stan.org. Accessed October 31, 2018.
32. Brooks SP, Gelman A (1998) General methods for monitoring convergence of iterative simulations. *J Comput Graph Stat* 7:434–455.